

Understanding the Blending Octane Behaviour of Unsaturated Hydrocarbons: A Case Study of C₄ Molecules and Comparison with Toluene

Yang Li^{*1}, Vijai Shankar Bhavani Shankar¹, Kiran K. Yalamanchi¹, Jihad Badra², André Nicolle³, S. Mani Sarathy¹

¹ King Abdullah University of Science and Technology, Clean Combustion Research Center, Thuwal 23955, Saudi Arabia

² Fuel Technology Division, R&DC, Saudi Aramco, Dhahran 31311, Saudi Arabia

³ Aramco Fuel Research Center, Aramco Overseas, Rueil-Malmaison 92500, France

Abstract

Octane number (ON) is an important empirical parameter for developing and optimizing internal combustion engine (ICE) for knock resistance. Primary reference fuels (PRF) comprising iso-octane and n-heptane are the simplest gasoline surrogates. C₄ hydrocarbons: butane isomers (n-butane and isobutane), butene isomers (1-butene, 2-butene and isobutene) and 1,3-butadiene are the smallest hydrocarbons with isomeric, saturated, unsaturated and conjugated bond structures, which makes them good candidates for understanding the blending octane behavior of saturated and unsaturated hydrocarbons. In this study, the blending octane behaviors of six PRF60 & C₄ hydrocarbon mixtures were systematically investigated. A state-of-the-art kinetic models were used by merging the latest KAUST gasoline surrogate model with the AramcoMech 3.0 model. IDTs of stoichiometric fuel/air mixtures were simulated at wide range of pressure (20 – 50 atm) and temperature (600 – 1400 K). Three correlation equations were employed from the literature to predict the research octane number (RON) and motor octane number (MON) of all blends based on these calculated IDTs. Compared with the experimentally measured ON, the best correlation conditions and errors were identified. With the highest degree of unsaturation, 1,3-butadiene was found to be the strongest ON enhancer. Moreover, based on a polynomial correlation, a TPRF (PRF + toluene) blend was formulated by matching the RON and MON of PRF plus 1,3-butadiene blend, for a comparative analysis. Finally, the reactants' consumption profile, flux and sensitivity analysis were simultaneously performed for explaining the chemistry behind the blending octane behavior of the PRF blends with 1,3-butadiene and toluene.

Keywords: Blending octane behavior; C₄ hydrocarbons; Ignition delay time; Research octane number; Motor octane number; Chemical kinetics

* Corresponding author: yang.li@kaust.edu.sa

31 **1. Introduction**

32 Octane number (ON) is an important indicator of the anti-knock quality of commercial gasoline
33 fuels. It is experimentally measured in a Cooperative Fuel Research (CFR) engine under two standard
34 operating procedures: ASTM D2699 [1] and ASTM D2700 [2], resulting in the research octane number
35 (RON) and motor octane number (MON) respectively. Primary reference fuels (PRF) is the simplest
36 surrogate used for representing a real gasoline fuel, which are binary blends of iso-octane and n-
37 heptane. By definition, the RON and MON values assigned for iso-octane and n-heptane are both 100
38 and 0 respectively. In addition, the difference and average values between the two properties are
39 defined as octane sensitivity ($S = \text{RON} - \text{MON}$) and anti-knock index ($\text{AKI} = (\text{RON} + \text{MON}) / 2$)
40 respectively. In order to match the octane sensitivity of a commercial fuel, toluene primary reference
41 fuel (TPRF) is another commonly used simple gasoline surrogate, which is a ternary mixture of PRF-
42 components and toluene. Toluene is a highly unsaturated hydrocarbon or aromatic hydrocarbon, with
43 the RON and MON values of 120 and 109 respectively [3].

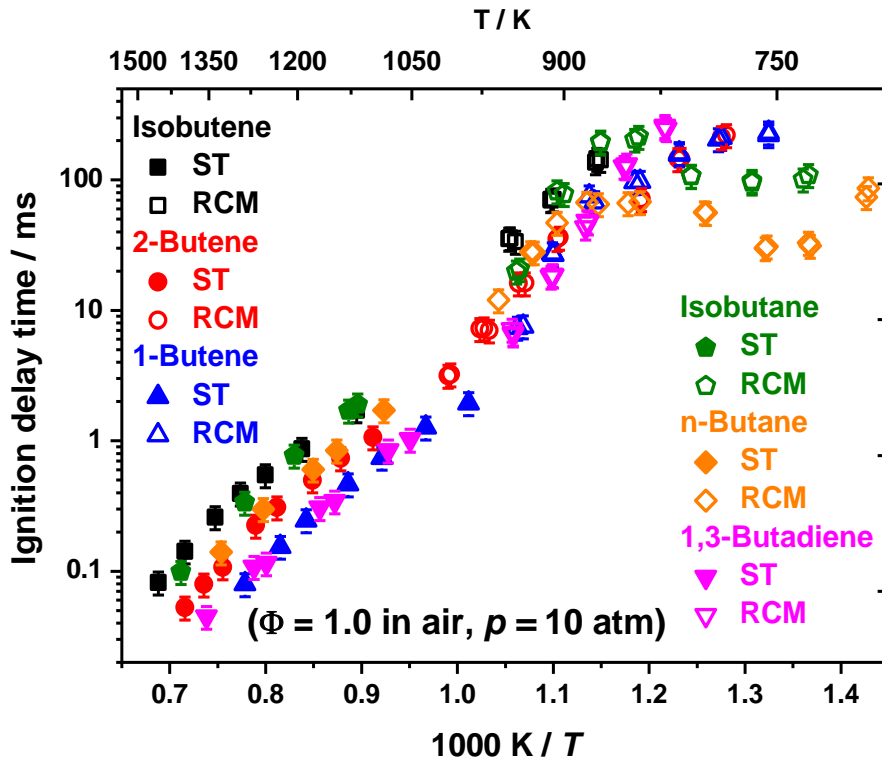
44 In general, for paraffinic PRF blends, S is equal to 0. While for other types of mixtures (molecules
45 with unsaturated structures or involving heteroatoms), S can be greater than 0, which is mainly
46 attributed to the significantly less pronounced negative temperature coefficient (NTC) behavior i.e.
47 their high resistance to auto-ignition under the test condition of RON than MON [4]. Therefore, the
48 blending octane behavior or knock propensity of a surrogate mixture is closely related to its
49 fundamental gas-phase oxidation chemistry. Recently, Andrae *et al.* [5] and Kang *et al.* [6] have
50 investigated the reactivity effect when adding the unsaturated and branched hydrocarbons
51 (diisobutylene) to PRF surrogate. C_4 hydrocarbons: butane isomers (n-butane and isobutane), butene
52 isomers (1-butene, 2-butene and isobutene) and 1,3-butadiene are the smallest hydrocarbons with both
53 isomeric and conjugated bond structures, which makes them good candidates for understanding the
54 blending octane behavior of unsaturated hydrocarbons by exploring their fundamental chemical
55 kinetics. Therefore, this aim of this study is four-fold:

- 56 • Use detailed chemical kinetic models to predict the IDTs of PRF plus C₄ hydrocarbon blends
57 at various temperature and pressure conditions
- 58 • Correlate the calculated IDTs with the octane number (RON and MON) at the optimal
59 temperature and pressure conditions
- 60 • Formulate the corresponding PRF plus toluene (TPRF) blends by matching the octane number
61 of PRF plus C₄ hydrocarbon blends
- 62 • Analyze and identify the important chemical kinetics behind the octane numbers of all PRF
63 plus C₄ hydrocarbon and TPRF blends

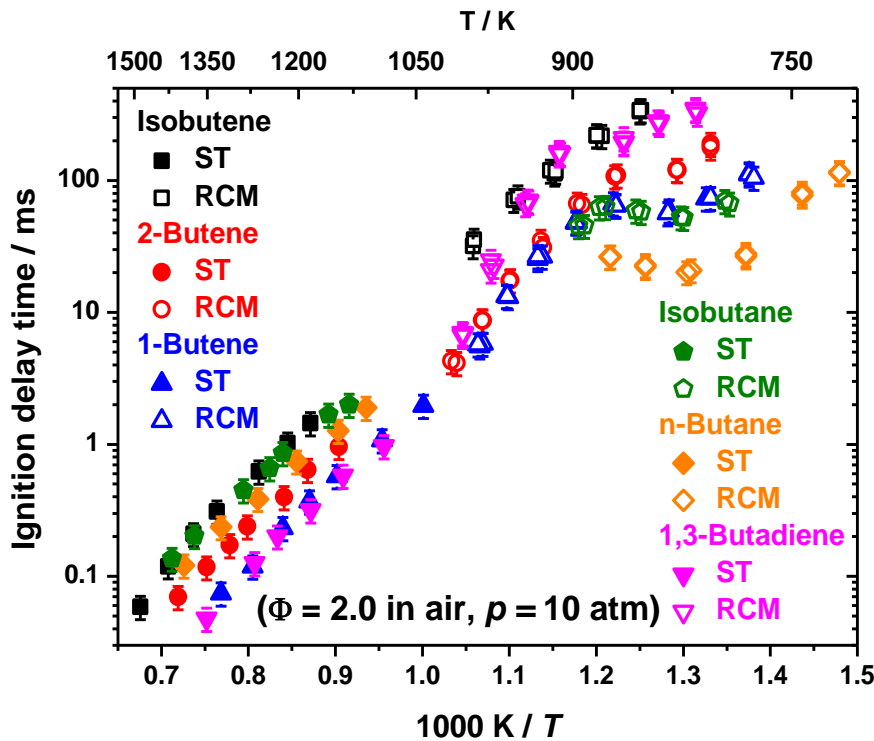
64 2. Ignition delay time comparisons

65 Ignition delay time (IDT) is an important indicator for evaluating the global reactivity of a fuel.
66 Some recent IDT measurements in shock tube (ST) and rapid compression machine (RCM) under
67 different conditions (equivalence ratio, pressure and temperature range) and detailed chemical kinetic
68 model studies of C₄ hydrocarbons oxidation are summarized in Table S1 in the Supplementary
69 Material 1. Figure 1 compares the IDTs of the six C₄ hydrocarbons under the two identical conditions:
70 (a) $\phi = 1.0$ and $p = 10$ atm; (b) $\phi = 2.0$ and $p = 10$ atm respectively. In the figure, different colors
71 represent the data for different species, and solid and open symbols correspond to the data taken from
72 ST and RCM respectively. It can be seen that the six species exhibit different IDTs because of the
73 difference in molecular structures. At high temperature (1000 – 1400 K), branched- and symmetric-
74 structured molecules (isobutane and isobutene) show longer IDTs than linear- and symmetric-
75 structured molecules (n-butane and 2-butene), with the linear- and asymmetric-structured molecule (1-
76 butene) and linear- and conjugated -structured molecule (1,3-butadiene) being the most reactive.
77 However, quantitatively, the difference between each other is only about a factor of two under the
78 same temperature. At low temperature (700 – 900 K), degrees of branching, symmetry and
79 unsaturation again play an important role on the ignition behavior of six species. The intensity of the
80 negative temperature coefficient (NTC) is roughly in this order: n-butane > isobutane > 1-butene > 2-
81 butene > isobutene \approx 1,3-butadiene. Molecules with higher degrees of linearity and longer length of

82 alkylic chain reveal stronger alkyl radical type low-temperature oxidation chemistry, which leads to
 83 more pronounced NTC behavior.



(a) $\phi = 1.0$



(b) $\phi = 2.0$

86
 87
 88 Figure 1. Ignition delay time comparison of C₄ hydrocarbons oxidation at 10 atm. n-Butane,
 89 isobutane, isobutene, 2-butene, 1-butene and 1,3-butadiene data are taken from Healy *et al.* [7],
 90 Healy *et al.* [8], Zhou *et al.* [9], Li *et al.* [10], Li *et al.* [11] and Zhou *et al.* [12] respectively.

91 3. Model validation and comparison

92 In this section, two recently developed detailed kinetic models are selected from literature for
93 estimating the IDTs of six C₄ hydrocarbons, their mixtures with PRF60 and TPRF blends. They are
94 named as AramcoMech 3.0 [12] and KAUST model [13] respectively, as summarized in Table 1. All
95 the models were well validated for IDT's of the containing species among C₄ hydrocarbons (butane
96 isomers, butene isomers and 1,3-butadiene) and TPRF components (iso-octane, n-heptane and toluene)
97 for a wide range of temperatures, pressures and equivalence ratios. In order to predict the IDTs of the
98 mixture of PRF60 plus C₄ hydrocarbons and TPRF blends, a new model was generated by merging
99 the KAUST and AramcoMech 3.0 mode. The model is named as KAUST_AramcoMech model and
100 contains 2317 species and 9699 reactions. The model in CHEMKIN format is provided in the
101 Supplementary Material 2.

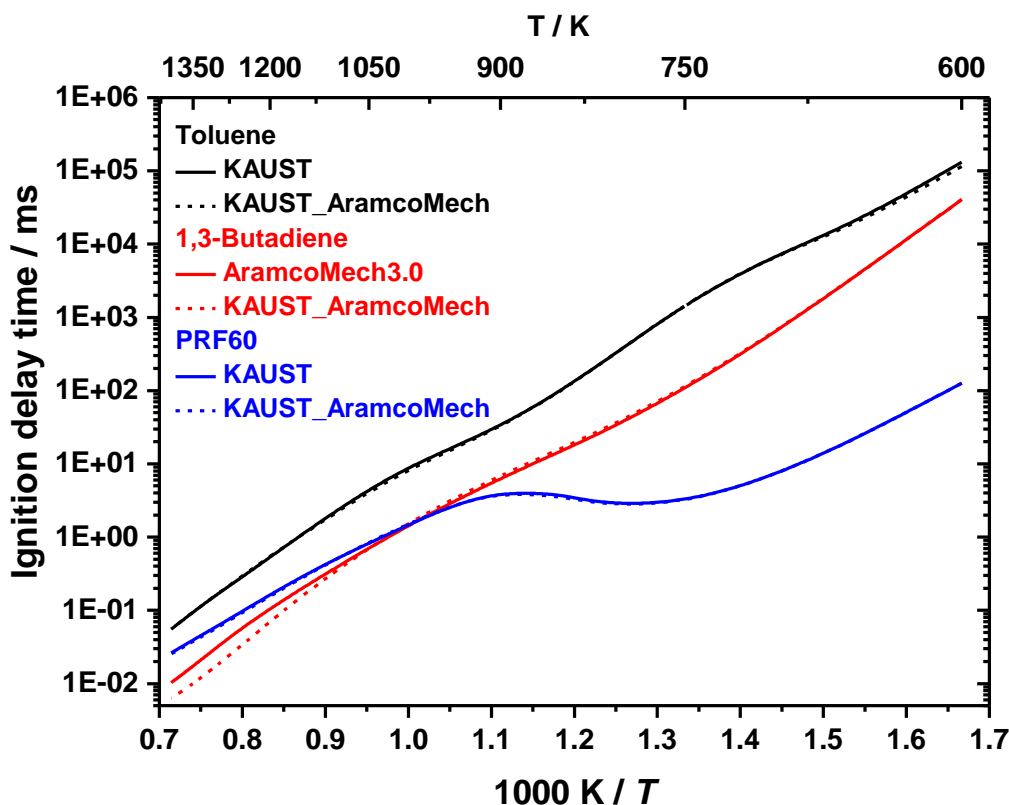
102 Table 1. Three kinetic models selected from literature.

NO.	Reference	Year	Name	Component
1	Zhou <i>et al.</i> [12]	2018	AramcoMech 3.0 model	All C ₄ hydrocarbons
2	Atef <i>et al.</i> [13]	2017	KAUST model	TPRF

103

104 It is worth mentioning that the original KAUST model [13] was developed on the basis of
105 AramcoMech 2.0 model [10]. Hence, merging was done by adding the updated 1,3-butadiene sub-
106 mechanism into the KAUST model. In order to confirm the accurate preservation of chemistry in the
107 merged model, the IDT simulation results were compared between the original models (KAUST and
108 AramcoMech 3.0 model) and merged model (KAUST_AramcoMech model) under the typical
109 condition of $\phi = 1.0$ and $p = 20$ atm, as shown in Figure 2. All IDT simulations, rate of production
110 (ROP), flux and sensitivity analysis were carried out using the ANSYS CHEMKIN- PRO [14]
111 software package. In the figure, different colors and line types denote different species and models,
112 respectively. Excellent repeatability was observed between the two models for all species (toluene,

113 1,3-butadiene and PRF60) across a wide range of temperatures, which testifies to the validity of the
114 merging process.



115

116

Figure 2. IDT comparisons between original models and merged model.

117

118

119

120

121

122

123

124

125

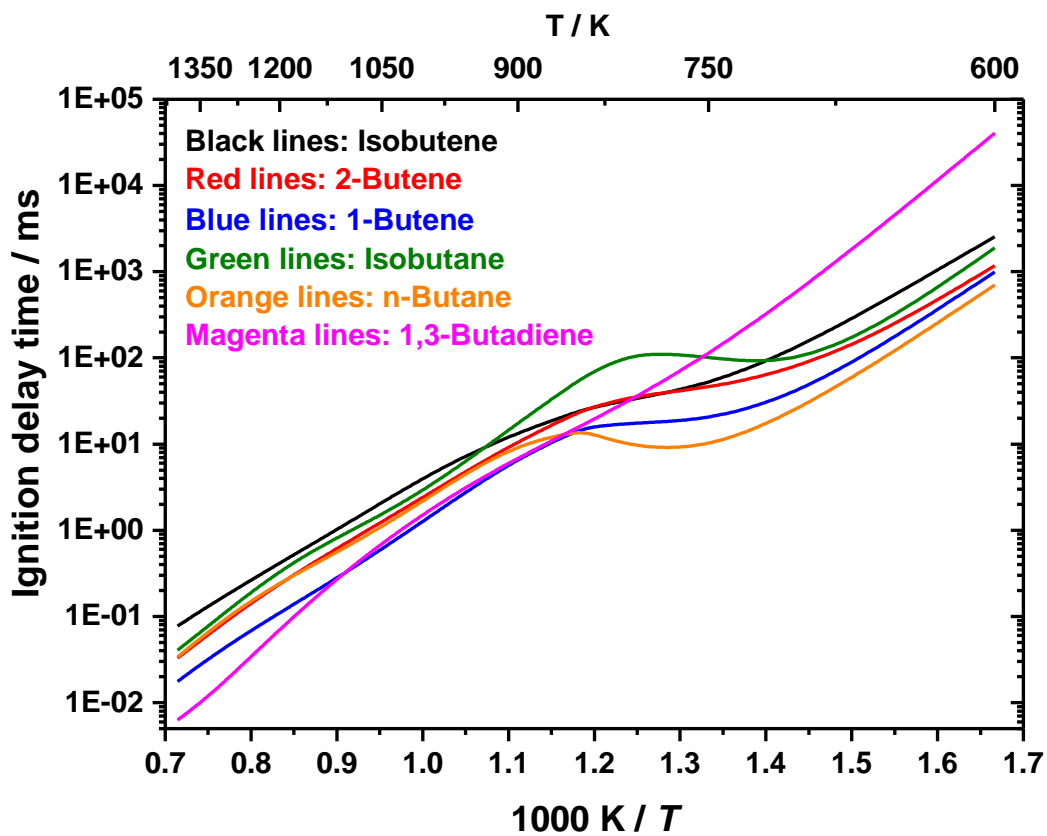
126

127

128

The merged model was then used to predict the IDTs of pure C₄ hydrocarbons and PRF60 plus C₄ hydrocarbons mixtures across wide range of pressures (20 – 50 atm) and temperatures (600 – 1400 K) extensively. All the simulations were performed with a constant volume batch reactor model at equivalence ratio of 1.0 and the pressure and temperature steps were set as 5 atm and 10 K, respectively. All data has been summarized in the Supplementary Material 3. Here, $p = 20$ atm and $T = 600 - 1400$ K case is taken as a representative to show the IDT/reactivity comparison of different blends, as shown in Figure 3. In the figure, different colors correspond to different reactants. Among the pure C₄ hydrocarbons, two saturated hydrocarbons: n-butane and isobutane show the most distinct NTC behavior. With the highest degree of unsaturation in the structure, 1,3-butadiene exhibits a linear relationship between its IDT and reciprocal of temperature, which results in a much longer IDT or lower reactivity towards low temperature (< 750 K) than all other C₄ hydrocarbons. This is also observed in the comparison of PRF60 plus C₄ hydrocarbons mixtures case, quantitatively, at the lowest

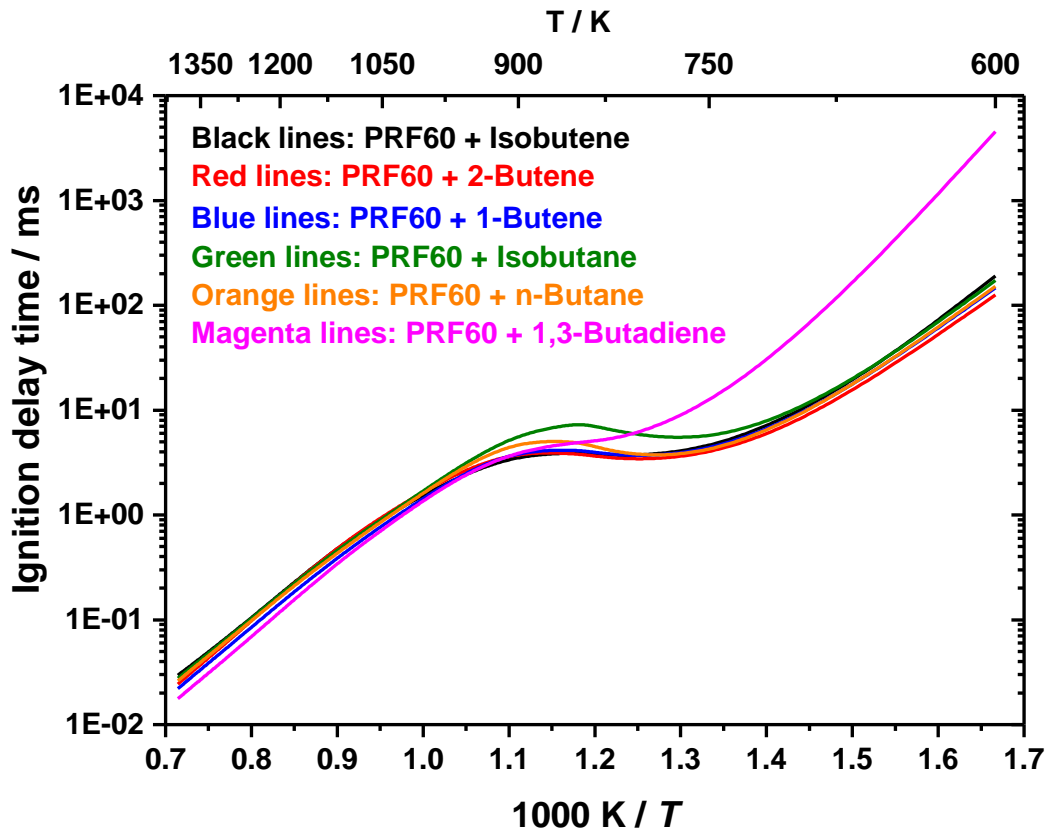
129 temperature being simulated (600 K) with the IDT difference between 1,3-butadiene and the rest of C₄
130 hydrocarbons is about a factor of 13.



131

132

(a) 100% C₄ hydrocarbons



(b) 80% PRF60 + 20% C₄ hydrocarbons

Figure 3. IDT comparisons for pure C₄ hydrocarbons and PRF60 plus C₄ hydrocarbons mixtures.

4. RON and MON predictions

Table 2 summarizes the octane numbers of all C₄ hydrocarbons and relevant mixtures, which were obtained from the American Society for Testing Materials (ASTM) [15], Puckett *et al.* [16], Clifford *et al.* [17], Boldt *et al.* [18] and Morganti *et al.* [19]. In the table, the RON and MON are shown for a) pure C₄ hydrocarbons; b) 80% PRF60 + 20% C₄ hydrocarbons; c) blending octane number. Here, PRF60 stands for the 60:40 mixture of iso-octane and n-heptane by volume, and the blending octane number (BON) is a hypothetical value obtained by extrapolating from the octane number of 20% concentration (by volume) of C₄ hydrocarbons to the value at 100% concentration. It can be seen that, in general, both RON and MON increase with the increasing degrees of branching and unsaturation, and 1,3-butadiene is found to be the strongest octane booster.

147
148

Table 2. Octane number of all C4 hydrocarbons and relevant mixtures (ASTM [15], Puckett *et al.* [16], Clifford *et al.* [17], Boldt *et al.* [18] and Morganti *et al.* [19]).

Species	100% C ₄	80% PRF60 + 20% C ₄	Blending octane number
RON			
n-Butane	93.5	70.6	113
iso-Butane	100.1	72.4	122
1-Butene	97.4	76.7	144
2-Butene	99.6	78.4	152
iso-Butene	-	81.9	170
1,3-Butadiene	-	87.1	196
MON			
n-Butane	89.0	70.7	114
iso-Butane	96.8	72.1	120
1-Butene	81.7	73.2	126
2-Butene	-	73.6	128
iso-Butene	-	75.8	139
1,3-Butadiene	-	76.8	144

149 In order to correlate the calculated IDTs in last section with the octane numbers shown in Table 2,
150 three sets of recently developed empirical equations were selected from literature: Badra *et al.* [20],
151 Singh *et al.* [21] and Naser *et al.* [22], and they were summarized in Table S3 in the Supplementary
152 Material 1. It is worth mentioning that all equations summarized in Table S3 were developed based on
153 the IDTs simulated under the identical pressure of 25 atm, however, these simulations were performed
154 using different kinetic models, different reactant mixtures and used different expressions (3-, 2-terms
155 natural logarithm, or exponential functions).

156 In this study, we employed all three sets of equations using the extensive IDTs obtained under wide
157 range of temperature and pressure conditions as input, both RON and MON of the six PRF60 + C₄
158 hydrocarbon blends were predicted based on the merged model: KAUST_AramcoMech, all results
159 were summarized in the Supplementary Material 3. Root Mean Squared Error (RMSE) was evaluated

160 between the octane numbers obtained from literature (shown in Table 2) and predicted using different
 161 equations based on the IDTs calculated by the merged kinetic model comprehensively for the PRF60
 162 and six PRF60 + C₄ hydrocarbons blends.

163 Table 3 shows the best correlation conditions and the corresponding RMSE errors for different
 164 equations and different kinetic models, for both RON and MON predictions. Overall, the RMSE errors
 165 were found to be within 7.0, which is quite small. In addition, these corrections were found to be more
 166 reliable at relatively lower pressures (20 and 25 atm) among the extensive pressures (20 – 50 atm)
 167 being investigated. Finally, the best correlation conditions were summarized as: (a) Badra *et al.* at the
 168 condition of $p = 25$ atm and $T = 760$ K; (b) Singh *et al.* at the condition of $p = 20$ atm and $T = 770$ K,
 169 therefore, they will be used for analyzing the fundamental chemistry in section 5.

170 Table 3. Best correlation conditions and the corresponding errors.

Correlation equations	Condition	Error
Badra <i>et al.</i>	$p = 25$ atm and $T = 760$ K	5.4 and 5.2
Singh <i>et al.</i>	$p = 20$ atm and $T = 770$ K	5.8 and 4.8
Naser <i>et al.</i>	$p = 20$ atm and $T = 740$ K	6.9 and 5.4

171 Among the six C₄ hydrocarbons, 1,3-butadiene with the conjugated bond structure, was found to be
 172 the strongest octane enhancer. Based on this, it would be interesting to see how a further increased
 173 degree of unsaturation of a hydrocarbon can affect its blending octane behavior with PRF. Toluene is
 174 a highly unsaturated hydrocarbon as well as a simple aromatic compound, which is also commonly
 175 used as an octane/sensitivity enhancer. Apart from the IDT-based correlation discussed above, Morgan
 176 *et al.* [3] and Kalghatgi *et al.* [23] have recently developed a second-order polynomial and linear-by-
 177 volume (LbV) correlations to map the composition of TPRF (PRF + toluene) surrogate based on the
 178 given RON and MON. Therefore, a TPRF blend was proposed by matching the octane number of the
 179 “80% PRF60 + 20% 1,3-Butadiene” mixture shown in Table 2. Table 4 shows the composition
 180 (volume ratio) and octane number of the two mixtures. It can be seen that TPRF blend has significantly
 181 higher amounts of iso-octane in PRF, and higher amount of toluene versus 1,3-butadiene, this clearly

182 indicates that 1,3-butadiene with less degree of unsaturation, has higher ability of boosting the octane
183 number than toluene. The detailed chemistry behind this will be discussed in the following section.

184

185 Table 4. The octane number and composition of PRF + 1,3-butadiene and PRF + toluene blends.

	80% PRF60 + 20% 1,3- Butadiene	TPRF
iso-Octane	48%	61.2%
n-Heptane	32%	7.9%
1,3-Butadiene	20%	-
Toluene	-	30.9%
RON	87.1	86.9
MON	76.8	77.0

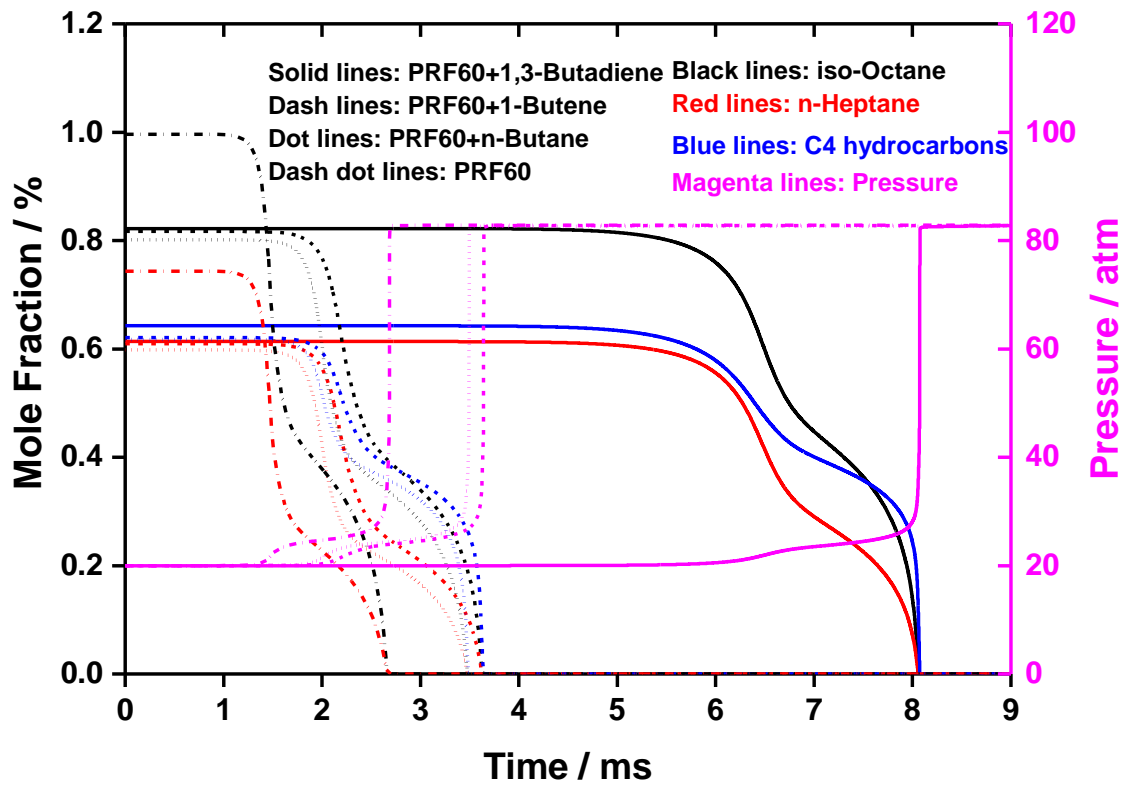
186

187 5. Chemical kinetics analyses

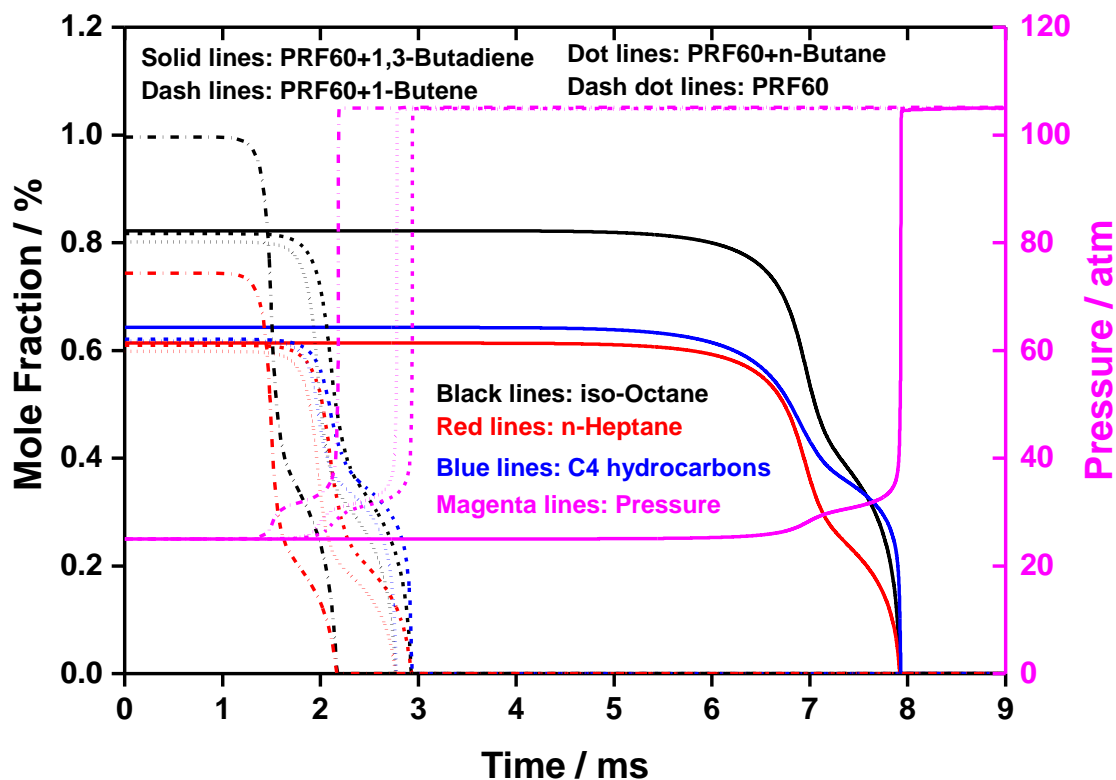
188 In order to investigate the chemistry behind the observed phenomena discussed in the last three
189 sections, the reactants' consumption profile, flux and sensitivity analyses were simultaneously
190 performed to identify the important chemical reactions for all six PRF60 plus C₄ hydrocarbon mixtures
191 as well as the TPRF blend. Firstly, we took the PRF60 and PRF60 + linear C₄ hydrocarbons (1,3-
192 butadiene, 1-butene and n-butane) blends as representatives, the rate of production (ROP) analysis was
193 performed using the merged model under the two best correlation conditions: (a) $p = 20$ atm and $T =$
194 770 K; (b) $p = 25$ atm and $T = 760$ K, as shown in Table 3. Figure 4 shows the reactants' consumption
195 profiles predicted for the reactants of the four mixtures. In the figure, different line types and colors
196 stand for different mixtures and the different components in each mixture respectively, and the pressure
197 traces are in magenta color corresponding to the y-axis at right side. All mixtures exhibit two-stage
198 ignition events which can be attributed to the low-temperature oxidation chemistry of saturated alkyl
199 radicals from iso-octane and n-heptane. PRF60 plus 1,3-butadiene blend exhibits the longest
200 consumption time (about 8 ms) among all mixtures. Therefore, flux analysis was performed for this

201 particular blend at the timing of the rapid decay of reactants after the first stage ignition, which is
202 around 7 ms.

203



(a) $p = 20$ atm and $T = 770$ K



(b) $p = 25$ atm and $T = 760$ K

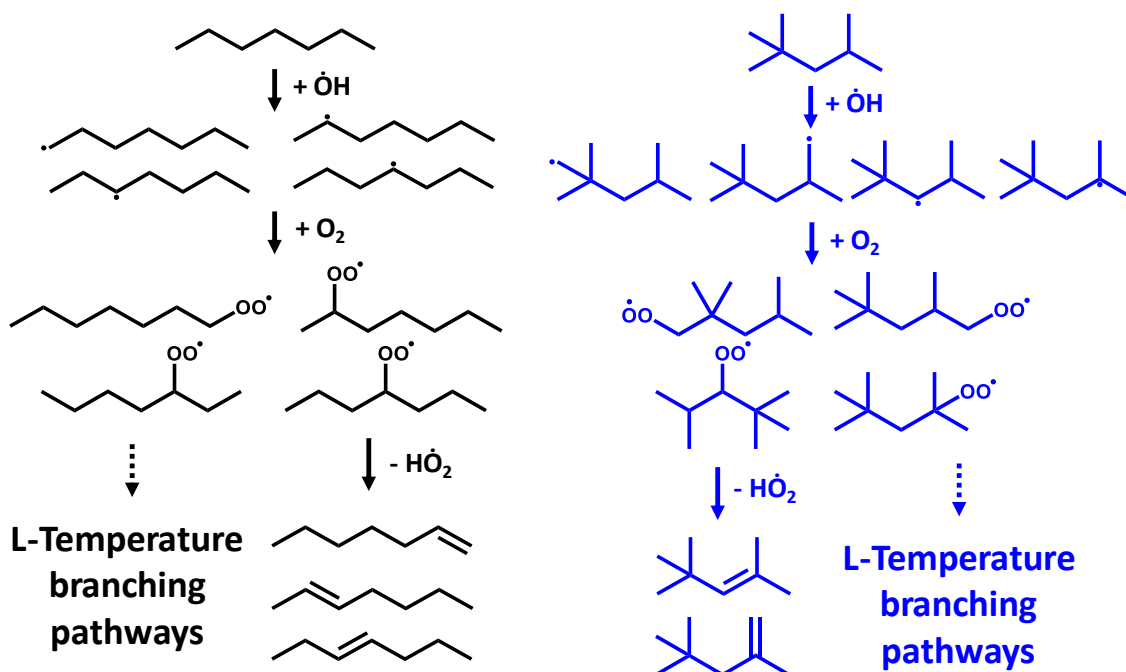
Figure 4. Reactants' consumption profile analysis for PRF60 and PRF60 plus C₄ hydrocarbon mixtures.

Figure 5 shows the flux analysis results for the PRF60 plus 1,3-butadiene blend, notably, in order to make the results more visualized, only the qualitative or generalized reaction pathways were exhibited in the figure, while the quantitative values for the flux of all reactions have been gathered in the Supplementary Material 4. As can be seen, both iso-octane and n-heptane exhibit typical alkyl radical low temperature chemistries, the competition between the HO_2 radical concerted elimination from RO_2 and RO_2 isomerization to QOOH leads to the NTC behavior. However, the oxidation chemistry of 1,3-butadiene is much more complex, fuel initiation chemistry contains two major reaction routes: (a) H-atom abstraction by $\dot{\text{O}}\text{H}$ radical; (b) $\dot{\text{O}}\text{H}$ radical addition to the C=C double bond, moreover, both routes can occur at two sides: terminal and central carbon atoms respectively. The abstraction reaction route generates two butadiene radicals (iso and normal), followed by the molecular oxygen or hydroperoxyl radical addition, while H-atom abstraction from the central carbon atom is

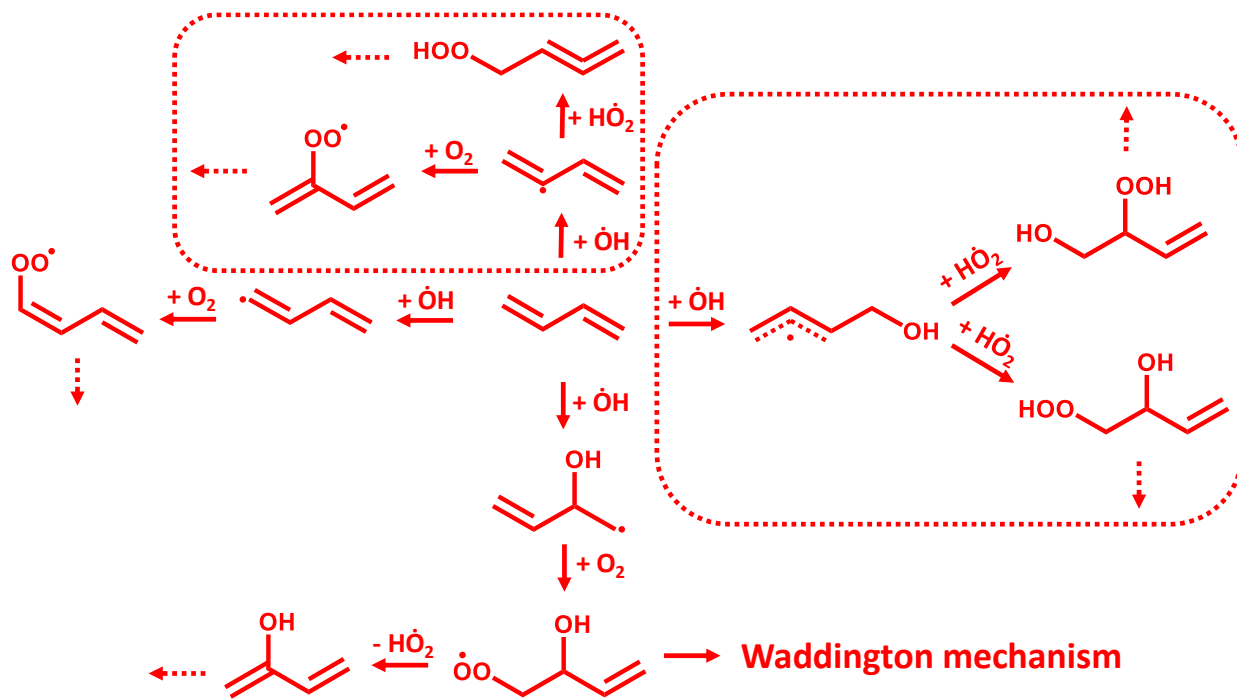
223 favored, since for the bond dissociation energy (BDE) of the C-H bond in 1,3-butadiene, secondary
 224 allylic-vinylic site ($101.5 \text{ kcal mol}^{-1}$) is significantly lower than primary vinylic site ($110.5 \text{ kcal mol}^{-1}$),
 225 which was calculated by Li *et al.* [24]. The addition reaction route is dominant at low temperature (T
 226 $< 900 \text{ K}$), however, $\dot{\text{O}}\text{H}$ radical adding to the terminal and central carbon atoms produce two different
 227 radicals, which further lead to two disparate reaction mechanisms. $\dot{\text{O}}\text{H}$ radical addition to the terminal
 228 carbon atom forms a resonantly-stabilized alcohol radical ($\text{C}_4\text{H}_6\text{4,2-1OH}$), which is a favored path
 229 inhibiting the reactivity, while central carbon addition reaction generates an alcoholic alkene radical
 230 ($\text{C}_2\text{H}_3\text{CHOHCH}_2$), which will subsequently undergo either $\text{H}\dot{\text{O}}_2$ radical concerted elimination or
 231 typical Waddington mechanism forming small aldehydes, ketones and $\dot{\text{O}}\text{H}$ radical.

232 To summarize, the two favored reaction pathways for the 1,3-butadiene oxidation have been
 233 circled/highlighted in Figure 5, both pathways inhibit the reactivity and consume vast amount of $\text{H}\dot{\text{O}}_2$
 234 radical during the radical propagation process. At the same time, the concerted elimination reaction of
 235 RO_2 radicals in PRF blend represents a major source $\text{H}\dot{\text{O}}_2$ radicals, therefore, the equilibrium of this
 236 reactivity inhibiting reaction would be shifted to the product side, which results in a second round
 237 reactivity inhibiting effects.

238



239



240

241 Figure 5. Major paths involved in the ignition of the PRF60 plus 1,3-butadiene blend ($p = 25$ atm, T
 242 $= 760$ K and $t = 7$ ms).

243

244

245

246

247

248

249

250

251

252

253

254

255

256

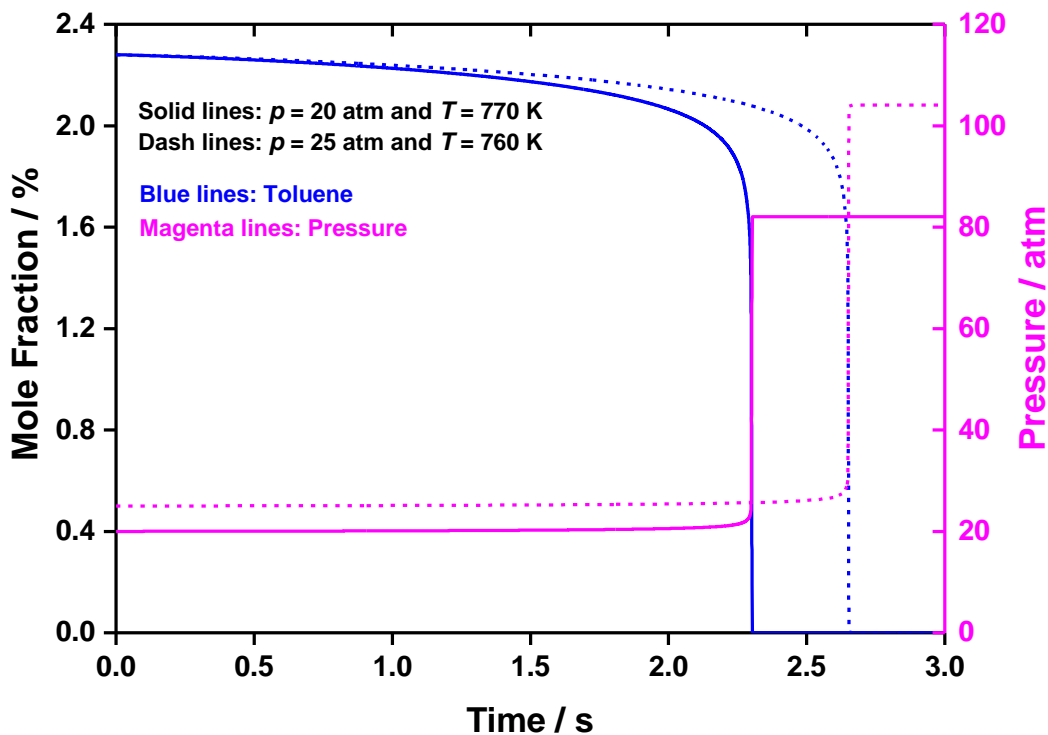
257

258

Furthermore, the reactants' consumption profile, flux and brute force sensitivity analysis [11] have all been carried out for both pure toluene and the proposed TPRF blend (shown in Table 4) under the two best conditions simultaneously. The reactants' consumption profile and sensitivity analysis were shown in Figure 6 and Figure 7 respectively. From the reactants' consumption profile, it can be seen that, after blending toluene with PRF, the two-stage ignition event was again clearly observed. In addition, the proposed TPRF blend predicts equivalent IDT (about 9 ms) with the "PRF60 plus 1,3-butadiene blend" at 25 atm and 760 K, which testified the reliability of the second-order polynomial correlation discussed in last section. From the sensitivity analysis, it can be seen that, the most inhibiting reaction is the fuel initiation chemistry: H-atom abstraction from the allylic H-atom on the methyl group by $\dot{\text{O}}\text{H}$ radical forming the benzyl radical ($\text{C}_6\text{H}_5\text{CH}_2\cdot$). Thereafter, the reactions between the formed benzyl radical ($\text{C}_6\text{H}_5\text{CH}_2\cdot$) and $\text{H}\dot{\text{O}}_2$ radical on the potential energy surface (PES) of $\text{C}_6\text{H}_5\text{CH}_2\text{OOH}$ took over the dominance, the association reaction forming benzyl-peroxy (BZCOOH) and chemical activation reaction forming benzoy radical ($\text{C}_6\text{H}_5\text{CH}_2\dot{\text{O}}$) plus $\dot{\text{O}}\text{H}$ radical became the top reactivity inhibiting and promoting reactions respectively. Of interest is that sensitivity analysis

259 results shows that by mixing the PRF with toluene, the main promoting reaction, namely allylic H-
 260 atom abstraction by molecular oxygen ($C_6H_5CH_3 + O_2 \leftrightarrow C_6H_5CH_2 + HO_2$) turned into an inhibiting
 261 reaction, as highlighted in red rounded rectangles.

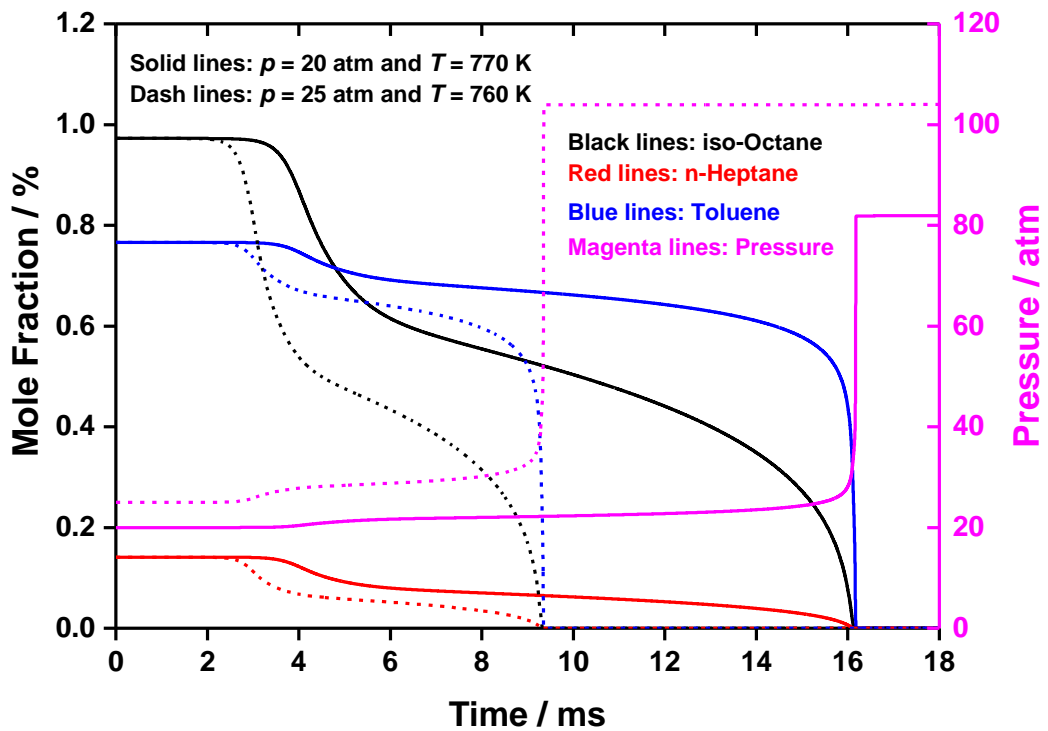
262



263

264

(a) Pure toluene



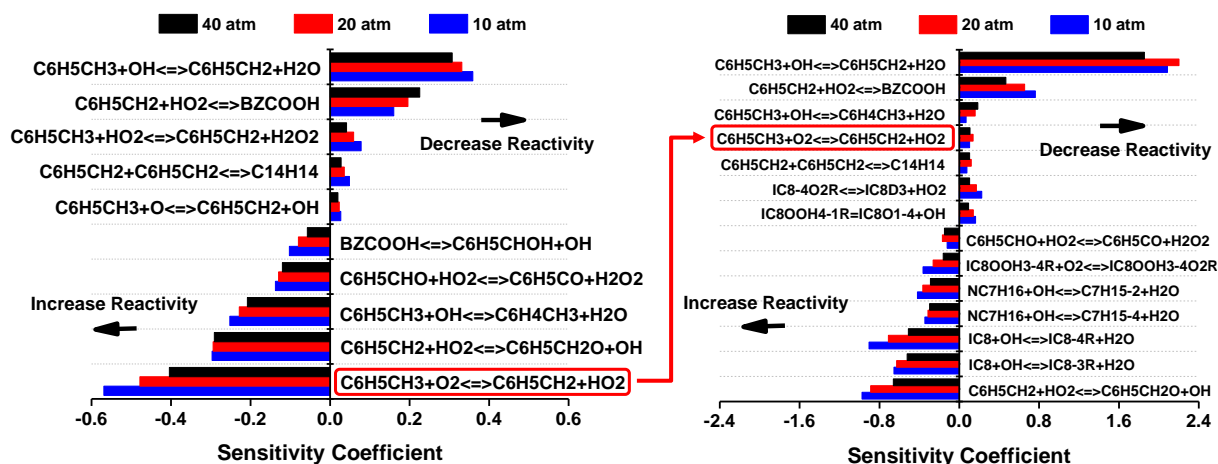
265

266

(b) TPRF blend

267

Figure 6. Reactants' consumption profile analysis for pure toluene and TPRF blend.



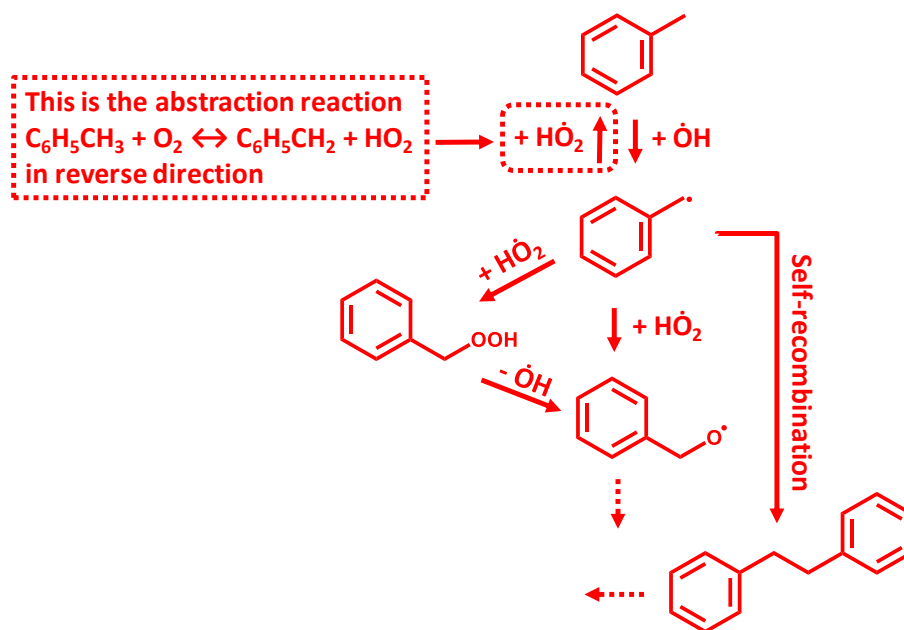
269

270

271

Figure 7. Sensitivity analysis for pure toluene and TPRF blend ($T = 760$ K).

272 Figure 8 shows the flux analysis results, which are the generalized reaction pathways for the toluene
 273 oxidation chemistry in the TPRF blend. It shows that this abstraction reaction actually occurs in the
 274 reverse direction. To summarize, by blending toluene with PRF, HO_2 radical can be sourced from the
 275 concerted elimination reaction of RO_2 radicals from the iso-octane and n-heptane oxidation. Then it
 276 reacts with benzyl radical ($\text{C}_6\text{H}_5\text{CH}_2$) via association or chemical activation reactions on the
 277 $\text{C}_6\text{H}_5\text{CH}_2\text{OOH}$ PES, or reacts reversely to give initial reactants (toluene and molecular oxygen), which
 278 is different from the 1,3-butadiene oxidation chemistry.



279

280 Figure 8. Flux analysis for the toluene oxidation chemistry in the TPRF blend ($p = 25$ atm, $T = 760$ K
 281 and $t = 4$ ms).

282 6. Conclusions

283 This study provided a systematic investigation of the blending octane behavior of C₄ hydrocarbons
284 (n-butane, isobutane, 1-butene, 2-butene, isobutene and 1,3-butadiene), as well as their comparison
285 with toluene. Investigations were carried by comparing experimentally measured RON and MON
286 obtained from literature with detailed chemical kinetic simulations. Empirical correlation equations
287 were employed to link fundamental chemistry with practical gasoline engine related octane numbers.
288 Below are some of the important findings:

- 289 • The two best correlations between the octane number and homogeneous IDTs are: (a) the
290 equations from Badra *et al.* at the condition of $p = 25$ atm and $T = 760$ K; (b) the equations
291 from Singh *et al.* at the condition of $p = 20$ atm and $T = 770$ K. The standard errors for both
292 are within 6.0.
- 293 • With the highest degree of unsaturation in its structure, 1,3-butadiene was found to be the
294 strongest octane enhancer among all C₄ hydrocarbons, and it is also stronger than toluene.
- 295 • On analyzing the oxidation chemistry behind above phenomenon, $\dot{\text{H}}\text{O}_2$ radical reacting with
296 allylic radical (C₄H₅-I, C₄H₆4,2-1OH and C₆H₅CH₂) plays a key role on the blending octane
297 behavior of unsaturated hydrocarbons. In 1,3-butadiene oxidation, the major reactivity
298 inhibiting reaction pathways are: $\dot{\text{O}}\text{H}$ radical addition to the terminal carbon atom and H-atom
299 abstraction from the central carbon atom. At the same time, the aforementioned reaction
300 pathways further inhibit oxidation pathways in PRF components, iso-octane and n-heptane,
301 namely: concerted elimination reaction of RO₂ radical forming the $\dot{\text{H}}\text{O}_2$ radical. In toluene
302 oxidation, $\dot{\text{H}}\text{O}_2$ radical was only involved in the reaction with the benzyl radical (C₆H₅CH₂);
303 however, three different reaction types were found to control its reactivity: (a) association
304 reaction forming the benzyl-peroxy (BZCOOH); (b) chemical activation reaction forming the
305 benzoxy radical (C₆H₅CH₂ $\dot{\text{O}}$) plus $\dot{\text{O}}\text{H}$; (c) reverse reaction of H-atom abstraction from methyl
306 group by molecular oxygen (C₆H₅CH₃ + O₂ ↔ C₆H₅CH₂ + HO₂).

307 From the application point of view, the merged kinetic model together with the correlations provide
308 a way of predicting the octane number when blending 1,3-butadiene with simple gasoline surrogates,
309 as well as understanding the interaction between olefins and alkanes in a commercial gasoline. At the
310 same time, understanding of the fundamental oxidation chemistry of highly unsaturated hydrocarbons
311 can be used for developing other relevant potential octane boosters in future.

312

313 **Acknowledgements**

314 The authors acknowledge the KAUST Supercomputing Laboratory (KSL) for providing the
315 computing resources and technical supports.

316

317 **Supplementary Material 1:** Additional information

318 **Supplementary Material 2:** Merged kinetic model

319 **Supplementary Material 3:** Calculated IDTs and ROM/MON correlations

320 **Supplementary Material 4:** Reactants' consumption profile and flux analysis results

321

322 **References**

- [1] D2699-19 Standard Test Method for Research Octane Number of Spark-Ignition Engine Fuel. West Conshohocken, PA; ASTM International, (2019).
- [2] D2700-19 Standard Test Method for Motor Octane Number of Spark-Ignition Engine Fuel. West Conshohocken, PA; ASTM International, (2019).
- [3] N. Morgan, A. Smallbone, A. Bhave, M. Kraft, R. Cracknell, G. Kalghatgi, Mapping surrogate gasoline compositions into RON/MON space, *Combustion and Flame*, 157 (2010) 1122-1131.
- [4] P. Pal, C.P. Kolodziej, S. Choi, S. Som, A. Broatch, J. Gomez-Soriano, Y. Wu, T. Lu, Y.C. See, in, SAE International, 2018.
- [5] J.C.G. Andrae, T. Kovács, Evaluation of Adding an Olefin to Mixtures of Primary Reference Fuels and Toluene To Model the Oxidation of a Fully Blended Gasoline, *Energy & Fuels*, 30 (2016) 7721-7730.
- [6] D. Kang, S. Kirby, J. Agudelo, M. Lapuerta, K. Al-Qurashi, A.L. Boehman, Combined Impact of Branching and Unsaturation on the Autoignition of Binary Blends in a Motored Engine, *Energy & Fuels*, 28 (2014) 7203-7215.
- [7] D. Healy, N.S. Donato, C.J. Aul, E.L. Petersen, C.M. Zinner, G. Bourque, H.J. Curran, n-Butane: Ignition delay measurements at high pressure and detailed chemical kinetic simulations, *Combustion and Flame*, 157 (2010) 1526-1539.
- [8] D. Healy, N.S. Donato, C.J. Aul, E.L. Petersen, C.M. Zinner, G. Bourque, H.J. Curran, Isobutane ignition delay time measurements at high pressure and detailed chemical kinetic simulations, *Combustion and Flame*, 157 (2010) 1540-1551.
- [9] C.-W. Zhou, Y. Li, E. O'Connor, K.P. Somers, S. Thion, C. Keese, O. Mathieu, E.L. Petersen, T.A. DeVerter, M.A. Oehlschlaeger, G. Kukkadapu, C.-J. Sung, M. Alrefae, F. Khaled, A. Farooq, P. Dirrenberger, P.-A. Glaude, F. Battin-Leclerc, J. Santner, Y. Ju, T. Held, F.M. Haas, F.L. Dryer, H.J. Curran, A comprehensive experimental and modeling study of isobutene oxidation, *Combustion and Flame*, 167 (2016) 353-379.
- [10] Y. Li, C.-W. Zhou, K.P. Somers, K. Zhang, H.J. Curran, The oxidation of 2-butene: A high pressure ignition delay, kinetic modeling study and reactivity comparison with isobutene and 1-butene, *Proceedings of the Combustion Institute*, 36 (2017) 403-411.

- [11] Y. Li, C.-W. Zhou, H.J. Curran, An extensive experimental and modeling study of 1-butene oxidation, *Combustion and Flame*, 181 (2017) 198-213.
- [12] C.-W. Zhou, Y. Li, U. Burke, C. Banyon, K.P. Somers, S. Ding, S. Khan, J.W. Hargis, T. Sikes, O. Mathieu, E.L. Petersen, M. AlAbbad, A. Farooq, Y. Pan, Y. Zhang, Z. Huang, J. Lopez, Z. Loparo, S.S. Vasu, H.J. Curran, An experimental and chemical kinetic modeling study of 1,3-butadiene combustion: Ignition delay time and laminar flame speed measurements, *Combustion and Flame*, 197 (2018) 423-438.
- [13] N. Atef, G. Kukkadapu, S.Y. Mohamed, M.A. Rashidi, C. Banyon, M. Mehl, K.A. Heufer, E.F. Nasir, A. Alfazazi, A.K. Das, C.K. Westbrook, W.J. Pitz, T. Lu, A. Farooq, C.-J. Sung, H.J. Curran, S.M. Sarathy, A comprehensive iso-octane combustion model with improved thermochemistry and chemical kinetics, *Combustion and Flame*, 178 (2017) 111-134.
- [14] ANSYS Chemkin-Pro 17.2, ANSYS, Inc.: San Diego, (2016).
- [15] Knocking Characteristics of Pure Hydrocarbons, American Society for Testing Materials, 1958.
- [16] A.D. Puckett, Knock ratings of gasoline substitutes, *Journal of Research of the National Bureau of Standards*, 35 (1945) 273-284.
- [17] E.A. Clifford, A practical guide to LP-gas utilization; LP-gas service & installation handbook, Moore Pub. Co., [New York, 1957.
- [18] K. Boldt, in, SAE International, 1967.
- [19] K. Morganti, T.M. Foong, M. Brear, G. Da Silva, Y. Yang, F. Dryer, in, SAE International, 2014.
- [20] J.A. Badra, N. Bokhumseen, N. Mulla, S.M. Sarathy, A. Farooq, G. Kalghatgi, P. Gaillard, A methodology to relate octane numbers of binary and ternary n-heptane, iso-octane and toluene mixtures with simulated ignition delay times, *Fuel*, 160 (2015) 458-469.
- [21] E. Singh, J. Badra, M. Mehl, S.M. Sarathy, Chemical Kinetic Insights into the Octane Number and Octane Sensitivity of Gasoline Surrogate Mixtures, *Energy & Fuels*, 31 (2017) 1945-1960.
- [22] N. Naser, S.M. Sarathy, S.H. Chung, Estimating fuel octane numbers from homogeneous gas-phase ignition delay times, *Combustion and Flame*, 188 (2018) 307-323.
- [23] G. Kalghatgi, H. Babiker, J. Badra, in, SAE International, 2015.
- [24] Y. Li, S.J. Klippenstein, C.-W. Zhou, H.J. Curran, Theoretical Kinetics Analysis for H Atom Addition to 1,3-Butadiene and Related Reactions on the $\dot{C}4H7$ Potential Energy Surface, *The Journal of Physical Chemistry A*, 121 (2017) 7433-7445.